Impact of topographic and atmospheric masses over Iran on validation and inversion of GOCE gradiometric data

Eshagh, M[1*]. and Sjöberg, L. E[2].

[1]*Ph.D student, Royal Institute of Technology, Stockholm, Sweden*
[2]*professor, Royal Institute of Technology, Stockholm, Sweden*

Abstract

The dedicated satellite mission GOCE will sense various small mass variations along its path around the Earth. Here we study the effect of the Earth's topography and atmosphere on GOCE data. The effects depend on the magnitude of topographic height, and they will therefore vary by region. As the effect of the atmosphere and topography must be removed from the total gravity anomaly prior to geoid determinations, these effects should also be removed to simplify the downward continuation of the GOCE data to the sea level.

The main goal of this article is to investigate the direct topographic and atmospheric effects in a rough region like Iran. Maps of the direct effects and their statistics are presented and discussed. Numerical results show maximum direct topographic and atmospheric effects on the GOCE data can reach 2.64 E and 5.53 mE, respectively, when the satellite flies over Iran. The indirect effect of the atmospheric and topographic masses are also formulated and presented.

Key words: Atmosphere, Satellite gradiometry, Topography, Topographic effect, Bias

اثر جرم‌های توپوگرافی و جوّی فراز ایران، بر ارزیابی و وارون‌سازی داده‌های گرادیومتری ماهواره گوس

مهدی اسحاق۱ و لارش اریک شوبرگ۲

۱ دانشجوی دکتری، مؤسسه سلطنتی صنعتی، استکهلم، سوئد
۲ استاد مؤسسه سلطنتی صنعتی، استکهلم، سوئد

چکیده

ماهوارهٔ گوس، در مأموریت در نظر گرفته شده، تغییرات کوچک جرم را در مسیر حرکت خود به دور زمین حس خواهد کرد. در این مقاله اثر توپوگرافی و جوّ زمین را روی داده‌های ماهواره گوس بررسی می‌کنیم. این اثرات به اندازه ارتفاعات توپوگرافی وابسته است و بنابراین، منطقه به منطقه تغییر می‌کند. از آنجا که اثرات جوّ و توپوگرافی از بی‌هنجاری جاذبه قبل از تعیین ژئوئید بایستی برداشته شود، این اثرات همچنین بایستی برای ساده کردن ادامه فروسوی داده‌های گوس روی تراز دریا نیز حذف و پس از ادامه فروسو، بازگردانده شوند. با توجه به اینکه داده‌های ماهواره گوس در ارتفاع ۲۵۰ کیلومتری زمین اندازه‌گیری می‌شود، با در نظر گرفتن سری هارمونیک‌های کروی خارجی و داخلی، می‌توان پتانسیل توپوگرافی را به‌صورت زیر در نظر گرفت.

Corresponding author: Tel: +4687907369   Fax: +4687907343   E-mail: eshagh@kth.se

$$V_{ext}^{t}(P) \doteq \frac{GM}{R}\sum_{n,m}^{\infty}\left(\frac{R}{r}\right)^{n+1}\left\{\frac{H_{nm}-N_{nm}}{R}+(n+2)\frac{H_{nm}^{2}-N_{nm}^{2}}{2R^{2}}+(n+2)(n+1)\frac{H_{nm}^{3}-N_{nm}^{3}}{6R^{3}}\right\}$$
$$\left[\frac{3\rho^{t}}{(2n+1)\rho^{e}}\right]Y_{nm}(P)$$

$$V_{int}^{t}(P) \doteq \frac{GM}{R}\sum_{n,m}^{\infty}\left(\frac{r}{R}\right)^{n}\left\{\frac{H_{nm}-N_{nm}}{R}-(n-1)\frac{H_{nm}^{2}-N_{nm}^{2}}{2R^{2}}+n(n-1)\frac{H_{nm}^{3}-N_{nm}^{3}}{6R^{3}}\right\}\left[\frac{3\rho^{t}}{(2n+1)\rho^{e}}\right]Y_{nm}(P)$$

در روابط بالا $V_{ext}^{t}(P)$ و $V_{int}^{t}(P)$ پتانسیل خارجی و داخلی توپوگرافی در هنگامی است که نقطه P خارج و داخل جرم‌های توپوگرافی قرار دارد، GM حاصل‌ضرب ثابت جهانی نیوتن و جرم زمین، R شعاع متوسط زمین، r فاصله ژئوسنتریک نقطه P، $\rho^{t}=26667kgm^{-3}$ چگالی متوسط توپوگرافی و $\rho^{e}=5500kgm^{-3}$ چگالی متوسط زمین، H_{nm}، H_{nm}^{2} و H_{nm}^{3} به ترتیب ضرایب هارمونیک کروی H، H^{2} و H^{3} هستند که در یک روند آنالیز هارمونیک ارتفاعات به‌دست می‌آیند. N_{nm}، N_{nm}^{2} و N_{nm}^{3} به ترتیب ضرایب هارمونیک N، N^{2} و N^{3} (N ارتفاع ژئوئید) و $Y_{nm}(P)$ نیز هارمونیک‌های کروی نرمال شده کامل است. همچنین بایاس توپوگرافی (تفاصل بین ادامه فروسوی پتانسیل خارجی و پتانسیل داخلی توپوگرافی روی سطح دریا) روی پتانسیل و بی‌هنجاری جاذبه نیز به‌صورت زیر مدل‌سازی می‌شود.

$$\delta V_{bias}^{t}(P) \doteq \frac{GM}{R}\sum_{n,m}^{\infty}\left[\frac{H_{nm}^{2}-N_{nm}^{2}}{2R^{2}}+\frac{H_{nm}^{3}-N_{nm}^{3}}{3R^{3}}\right]\left(\frac{3\rho^{t}}{\rho^{e}}\right)Y_{nm}(P)$$

$$\delta\Delta g_{bias}^{t}(P) \doteq \frac{GM}{R^{2}}\sum_{n,m}^{\infty}\left[\frac{H_{nm}-N_{nm}}{R}+(n-1)(n+2)\frac{H_{nm}^{3}-N_{nm}^{3}}{6R^{3}}\right]\left(\frac{3\rho^{t}}{\rho^{e}}\right)Y_{nm}(P)$$

با فرض جوّ ساکن و اینکه چگالی جوّ فقط در ارتفاع متغییر است، نواک (۲۰۰۰) مدل زیر را براساس یک برازش ساده به مدل استاندارد جوّ امریکا در سال ۱۹۷۶ منتشر شد ارائه کرد. همان‌طور که وی نیز اشاره کرده است، این مدل فقط تا ارتفاع ده کیلومتری از سطح دریا قابل استفاده است و اثر جرم‌های جوّ بالای این ارتفاع باید جداگانه بررسی شود.

$$\rho(r) = \rho_{0}\left[1+\alpha'(r-R)+\beta'(r-R)^{2}\right]$$

در این رابطه $\rho_{0}=1.2227kgm^{-3}$ و $\beta'=2.2781\times10^{-9}\left(m^{-2}\right)$ و $\alpha'=-7.6495\times10^{-5}\left(m^{-1}\right)$ چگالی جوّ در سطح دریاها است. پتانسیل خارجی و داخلی جوّ براساس این مدل برحسب سری هارمونیک‌های کروی به‌صورت زیر است

$$V_{ext}^{a}(P) \doteq \frac{GM}{R}\sum_{n,m}^{\infty}\left(\frac{R}{r}\right)^{n+1}\left[\frac{Z_{nm}-H_{nm}}{R}+(n+2-\alpha'R)\frac{Z_{nm}^{2}-H_{nm}^{2}}{2R^{2}}\right.$$
$$\left.+\left[(n+2)(n+1-2\alpha'R)+2\beta'R^{2}\right]\frac{Z_{nm}^{3}-H_{nm}^{3}}{6R^{3}}\right]\left[\frac{3\rho_{0}}{(2n+1)\rho^{e}}\right]Y_{nm}(P)$$

$$V_{int}^{a}(P) \doteq \frac{GM}{R}\sum_{n,m}^{\infty}\left(\frac{r}{R}\right)^{n}\left[\frac{Z_{nm}-H_{nm}}{R}-(n-1-\alpha'R)\frac{Z_{nm}^{2}-H_{nm}^{2}}{2R^{2}}\right.$$
$$\left.+\left[(1-n)(n+2\alpha'R)-2\beta'R^{2}\right]\frac{Z_{nm}^{3}-H_{nm}^{3}}{6R^{3}}\right]\left[\frac{3\rho_{0}}{(2n+1)\rho^{e}}\right]Y_{nm}(P)$$

در این روابط Z_{nm} حد بالای جوّ در مدل و برابر ۱۰ کیلومتر است. از آنجا که این مقداری ثابت است، بنابراین پتانسیل فقط در هارمونیک درجه صفر، نقش خواهد داشت. به ترتیب مشابه بایاس جوّی نیز روی پتانسیل اتمسفر و بی‌هنجاری جاذبه به‌صورت زیر مدل‌سازی می‌شود.

$$\delta\Delta g^{t}_{bias}(P) \doteq \frac{GM}{R^2}\sum_{n,m}^{\infty}\left\{\frac{Z_{nm}-H_{nm}}{R}+\frac{3\alpha'R}{(2n+1)}\frac{Z^2_{nm}-H^2_{nm}}{2R^2}+\frac{Z^3_{nm}-H^3_{nm}}{6R^3}\Big[(n+2)(n-1)+2\beta R^2\Big]\right\}$$
$$\left(\frac{3\rho_0}{\rho^e}\right)Y_{nm}(P)$$

$$\delta V^{a}_{bias}(P) \doteq \frac{GM}{R}\sum_{n,m}^{\infty}\left\{(2n+1-2\alpha'R)\frac{Z^2_{nm}-H^2_{nm}}{2R^2}+\frac{Z^3_{nm}-H^3_{nm}}{3R^3}\Big[(n^2+n+1)-3\alpha'R+2\beta'R^2\Big]\right\}$$
$$\left[\frac{3\rho_0}{(2n+1)\rho^e}\right]Y_{nm}(P)$$

به منظور در نظر گرفتن اثر جرم‌های جوّی بالاتز از ارتفاع ده کیلومتر، روابط زیر برای پتانسیل داخلی و خارجی مانند یک جمله تصحیحی به هارمونیک درجه صفر این بسط ارائه می‌شود

$$\left(\delta V^{a}_{ext}\right)_0=\frac{3}{\rho^e}\left\{\left(1+\frac{Z_{j+1}}{R}\right)^3\rho^a_j-\left(1+\frac{Z_i}{R}\right)^3\rho^a_i+\sum_{k=i+1}^{j}\left(1+\frac{Z_k}{R}\right)^3\left(\rho^a_{k-1}-\rho^a_k\right)\right\}$$

$$\left(\delta V^{a}_{int}\right)_0=\frac{3}{2\rho^e}\left\{\left(1+\frac{Z_{j+1}}{R}\right)^2\rho^a_j-\left(1+\frac{Z_i}{R}\right)^2\rho^a_i+\sum_{k=i+1}^{j}\left(1+\frac{Z_k}{R}\right)^2\left(\rho^a_{k-1}-\rho^a_k\right)\right\}$$

با تقسیم جوّ بالای این ارتفاع به لایه‌های ۱۰۰ متری و محاسبه چگالی درون هر لایه با میانگین بین حد بالا و پایین لایه، می‌توان پتانسیل جوّ از ارتفاع ۱۰ تا ارتفاع ۸۶ کیلومتری را به راحتی با روابط فوق محاسبه کرد. در این روابط، i شماره اولین لایه و j شماره لایه آخر است. Z ها نیز بیانگر حد بالا و پایین لایه ها و ρ ها نیز چگالی جوّ در هر لایه است.

پس از بهدست آوردن ضرایب هارمونیک‌های کروی پتانسیل توپوگرافی و جوّ کافی است که این ضرایب در روابط معروف بیان هارمونیکی دادهای گرادیومتری بهجای هارمونیک‌های میدان جاذبه زمین گذارنده شود تا اثرات روی دادهای گرادیومتری گوس محاسبه شود. در این مقاله بهمنظور محاسبه اثرات، روابط غیر تکین ارائه شده پتروسکایا و ورشکو (۲۰۰۶) در دستگاه مختصات محلی استفاده شده است. اعداد و آمارهای اثر توپوگرافی و جوّ در ایران روی دادهای ماهواره گوس در جدول زیر ارائه می‌شود.

جدول ۱. اثر توپوگرافی و جوّ روی دادهای گوس در منطقه ایران.

	اثر جوّ (میلی اتووش)				اثر توپوگرافی (اتووش)			
	انحراف معیار	کمترین	میانگین	بیشترین	انحراف معیار	کمترین	میانگین	بیشترین
V_{xx}	± 0.35	-2.86	-2.23	-1.20	± 0.68	-2.60	-0.65	0.59
V_{yy}	± 0.25	-3.16	-2.59	-1.97	± 0.48	-1.16	0.01	1.06
V_{zz}	± 0.48	3.78	4.82	5.53	± 0.94	-0.76	0.64	2.64
V_{xy}	± 0.21	-0.50	0.07	0.45	± 0.41	-0.89	-0.14	0.98
V_{xz}	± 0.47	-0.89	0.06	0.99	± 0.92	-1.94	-0.10	1.72
V_{yz}	± 0.30	-0.91	-0.10	0.70	± 0.58	-1.35	0.20	1.69

همان‌طور که در جدول بالا مشاهده می‌شود، بیشترین اثر توپوگرافی 2.64 اتووش است، در حالی‌که بیشترین اثر جوّ در ایران حدود 5.53 میلی اتووش ثبت شده است. بیشترین اثرات مربوط به کمیت V_{zz} است و کمترین آن مربوط به V_{xy} از آنجا که در بسط

هارمونیک V_{zz} شامل هارمونیک درجه صفر و یک است در حالی‌که V_{xy} فاقد این ضرایب هارمونیک است، تعبیر فیزیکی این اثرات

نیز در مقاله اشاره شده است.

واژه‌های کلیدی: جوّ، گرادیومتری ماهواره‌ای، توپوگرافی، اثر توپوگرافی، بایاس

1 INTRODUCTION

The geoid, when representing the physical shape of the Earth, plays an important role as a vertical datum. In order to compute the geoid, the gravity field of the Earth should be known. The geoid can be divided into its long-wavelength and short-wavelength parts. The former is most successfully determined from satellite observations, and it is usually represented globally by an Earth Gravity Model (EGM), i.e. a low-degree and -order set of spherical harmonics. The short-wavelength part is usually determined from regional gravity data by the classical Stokes formula. Various forms of modifying Stokes' formula exist with the general goal of reducing the truncation error made by limiting the Stokes integration area around the computation point, and the limited set of the EGM. In addition, the least squares modification of Stokes' formula, presented by Sjöberg (1984, 1986 and 1991), matches the errors stemming from truncation, the EGM and the gravity data used in the Stokes integration in an optimum way.

Classically the long-wavelength part of the gravity field is determined by dynamic satellite geodesy, which means that the perturbations of the satellite orbit are interpreted in terms of perturbing harmonics of the Earth's gravity field. The recent dedicated satellite missions, like CHAMP, GRACE and near future GOCE improve and will improve the quality of most coefficients and will also extend the upper limit of the EGM to nearly degree and order 300. This will particularly be the case from the high sensitivity data of GOCE. Also in satellite gradiometry there are two main approaches to be considered: the time-wise and space-wise approaches (Rummel et al. 1993). The time-wise approach was developed, e.g., by Koop (1993), and various forms of this approach were further developed, e.g., by Sneeuw (1992 and 2000), Klees et al. (2000), Sneeuw et al. (2001). In the space-wise approach the geopotential coefficients are determined from the second order derivatives of the gravity potential (Rummel et al. 1993), and Petrovskaya and Vershkov (2006) choose the local north-oriented reference frame to present the gradients in terms of geopotential spherical harmonic coefficients. Martinec (2003) has solved the gradiometric boundary value problem using tensor spherical harmonics. Ditmar et al. (2003) also considered the large amount of data involved in the computations, calling for fast and accurate algorithms.

The effects of topography and atmosphere on satellite gravimetry and gradiometry were previously investigated by Novák and Grafarend (2006). Knowing the gravitational potential generated by topography and atmosphere allows us to remove these effects from the geopotential. In a no-topography and no-atmosphere space it is simpler to downward continue the satellite gradiometric data. As an alternative one can use analytical continuation and consider the total effect on the downward continued data. In downward continuation six partial derivatives of the Stokes or Abel-Poisson integral can be used; see Reed (1973), Rummel (1975) and also Novák (2007). The result will be the downward continued gravity anomaly or disturbing potential. The topographic and atmospheric masses also play an important role in precise validation and calibration of GOCE data.

In the present article we consider the effects of topographic and atmospheric masses on satellite gradiometric data (direct effects) as well as downward continued gravity anomaly and disturbing potential (indirect effects). The paper considers the atmospheric potential based on the United States atmospheric density model (United State Standard Atmosphere, 1976).

In section 2 we discuss theoretically the topographic potential in spherical harmonics and the atmospheric potential in spherical harmonics is investigated in section 3. In section 4 non-singular expressions of the gradients are given. section 5 deals with a numerical study in Iranian territory on the direct atmospheric effect on the GOCE gradiometric data, and, finally, in Section 6 some conclusions are presented.

2 TOPOGRAPHIC POTENTIAL IN SPHERICAL HARMONICS

Our definition of the topography is the masses between the geoid and the surface of the Earth

(Novák and Grafarend, 2006). The gravitational potential $V(P)$ is harmonic and can be expanded into an external harmonics series (and, in particular, at satellite level):

$$V_{ext}^t(P) = \frac{GM}{R}\sum_{n,m}^{\infty}\left(\frac{R}{r}\right)^{n+1}\left(V_{ext}^t\right)_{nm} Y_{nm}(P)$$

(1)

where GM is the product of gravitational constant and Earth's mass, R is the selected mean radius of sea level. r is the geocentric distance. Superscript's stands for topography, and

$$Y_{n,m}(P) = \overline{P}_{n,|m|}(\cos\theta)Q_m(\lambda),$$

(2)

is the fully-normalized spherical harmonics with

$$Q_m(\lambda) = \begin{cases} \cos m\lambda, & m \geq 0 \\ \sin|m|\lambda, & m < 0 \end{cases},$$

(3)

$$\sum_{n,m}^{\infty} = \sum_{n=0}^{\infty}\sum_{m=-n}^{n}$$

and $\overline{P}_{n,|m|}$ is the fully-normalized associated Legendre function, θ and λ are the co-latitude and longitude, respectively. The $\left(V_{ext}^t\right)_{nm}$ is the spherical harmonic coefficient of the topographic potential, that can be presented as

$$\left(V_{ext}^t\right)_{nm} = \frac{3}{2n+1}\frac{\rho^t}{\rho^e}\left(F_{ext}^t\right)_{nm}$$

(4)

where, $\rho^t = 2.6667\ \mathrm{kg\,m^{-3}}$ is the mean density of the topography and $\rho^e \doteq 5500\ \mathrm{kg\,m^{-3}}$ is the mean density of the Earth's mass, $\left(F_{ext}^t\right)_{nm}$ is approximated as (Novák and Grafarend, 2006)

$$\left(F_{ext}^t\right)_{nm} \doteq \frac{H_{nm} - N_{nm}}{R} + (n+2)\frac{H_{nm}^2 - N_{nm}^2}{2R^2} + \\ + (n+2)(n+1)\frac{H_{nm}^3 - N_{nm}^3}{6R^3},$$

(5)

where H_{nm}, H_{nm}^2, H_{nm}^3, N_{nm}, N_{nm}^2 and N_{nm}^3 are the spherical harmonics of H, H^2, H^3, N, N^2 and N^3, respectively. These coefficients can

be obtained by a general spherical harmonic analysis (GSHA) of a global digital elevation model (DEM) such as GTOPO or SRTM (Wieczorek, 2007), and the EGM96 geopotential model (Lemoine et al. 1998).

The indirect effect can also be written

$$V_{int}^t(P) = \frac{GM}{R}\sum_{n,m}^{\infty}\left(\frac{r}{R}\right)^n\left(V_{int}^t\right)_{nm} Y_{nm}(P),$$

(6)

where

$$\left(V_{int}^t\right)_{nm} = \frac{3}{2n+1}\frac{\rho^t}{\rho^e}\left(F_{int}^t\right)_{nm},$$

(7)

and

$$\left(F_{int}^t\right)_{nm} \doteq \frac{H_{nm} - N_{nm}}{R} - (n-1)\frac{H_{nm}^2 - N_{nm}^2}{2R^2} + \\ + n(n-1)\frac{H_{nm}^3 - N_{nm}^3}{6R^3}.$$

(8)

for $r \leq R$. The direct and indirect effects are used in the remove-compute-restore technique. However, when analytical continuation is considered one can perform downward continuation disregarding these effects and add the total effect (a combination of direct and indirect effects) on the downward continued quantities. As mentioned in the introduction the downward continued quantities are the gravity anomaly or geoid. Based on the fundamental theorem of physical geodesy (Heiskanen and Moritz, 1967) we have

$$\delta\Delta g(P) = -\frac{\partial V(P)}{\partial r} - \frac{2}{r}V(P),$$

(9)

where $V(P)$ is either external or internal topographic potential. Therefore the direct and indirect effect on the gravity anomaly will be

$$\delta\Delta g_{ext}^t(P) = \frac{GM}{R^2}\sum_{n,m}^{\infty}(n-1)\left(\frac{R}{r}\right)^{n+1}\left(V_{ext}^t\right)_{nm} \\ Y_{nm}(P),$$

(10)

$$\delta\Delta g_{int}^t(P) = -\frac{GM}{R^2}\sum_{n,m}^{\infty}(n+1)\left(\frac{r}{R}\right)^{n-1}\left(V_{int}^t\right)_{nm} \\ Y_{nm}(P),$$

(11)

The topographic bias (or the total effect) on the gravity anomaly will be:

$$\delta\Delta g_{bias}^{t}\left(P\right)=\left[\delta\Delta g_{ext}^{t}\left(r,\Omega\right)\right]^{*}- -\delta\Delta g_{int}^{t}\left(r,\Omega\right)\Big|_{r=R}. \quad (12)$$

Inserting equation (10) and equation (11) for r=R into Equation (9) yields

$$\delta\Delta g_{bias}^{t}\left(P\right)\doteq\frac{GM}{R^{2}}\sum_{n,m}^{\infty}\left[\frac{H_{nm}-N_{nm}}{R}+\left(n-1\right)\left(n+2\right)\times \frac{H_{nm}^{3}-N_{nm}^{3}}{6R^{3}}\right]\left(\frac{3\rho^{t}}{\rho^{e}}\right)Y_{nm}\left(P\right). \quad (13)$$

In a similar way as in equation (12) we can write the topographic bias on the disturbing potential as:

$$\delta V_{bias}^{t}\left(P\right)\doteq\frac{GM}{R}\sum_{n,m}^{\infty}\left[\frac{H_{nm}^{2}-N_{nm}^{2}}{2R^{2}}+\frac{H_{nm}^{3}-N_{nm}^{3}}{3R^{3}}\right]\left(\frac{3\rho^{t}}{\rho^{e}}\right)Y_{nm}\left(P\right), \quad (14)$$

which is the same as the topographic bias in Sjöberg (2007).

3 ATMOSPHERIC POTENTIAL IN SPHERICAL HARMONICS

Generally, a spherical approximation of sea level of the Earth and no atmosphere outside a sphere extending 86 km above sea level (maximum height considered in the standard atmospheric model; see Appendix B) is assumed. As Ecker and Mittemayer (1969) presented, more than 99% of the atmospheric masses are included up to the elevation of 50 km. This is why some users select this level as the upper bound of the atmospheric masses (see e.g., Novák and Grafarend 2006). However, Wallace and Hobbs (1977) believe that this value is at 30 km and also Lambeck (1988) mentioned that 80% of the atmospheric masses are below 12 km; therefore Novák's (2000) proposition to consider a simple polynomial to formulate the atmospheric density below 10 km height is not so far from reality. This polynomial is:

$$\rho\left(r\right)=\rho_{0}+\alpha\left(r-R\right)+\beta\left(r-R\right)^{2}. \quad (15a)$$

where

$$\alpha=-1.1436\times10^{-4}\left(m^{-1}\right) \quad (15b)$$

$$\beta=+3.4057\times10^{-9}\left(m^{-2}\right). \quad (15c)$$

This model can also be written as

$$\rho\left(r\right)=\rho_{0}\left[1+\alpha'\left(r-R\right)+\beta'\left(r-R\right)^{2}\right], \quad (16a)$$

where

$$\alpha'=-7.6495\times10^{-5}\left(m^{-1}\right) \quad (16b)$$

$$\beta'=2.2781\times10^{-9},\left(m^{-2}\right). \quad (16c)$$

Based on Equation (16a) the external atmospheric potential can easily be formulated using a Newtonian integral and spherical harmonics. In this case we can write the spherical harmonic coefficients of the atmospheric potential as (Novák and Grafarend, 2006):

$$\left(V_{ext}^{a}\right)_{nm}=\frac{3}{2n+1}\frac{\rho^{a}}{\rho^{e}}\left(F_{ext}^{a}\right)_{nm}, \quad (17)$$

where

$$\left(F_{ext}^{a}\right)_{nm}\doteq\frac{Z_{nm}-H_{nm}}{R}+\left(n+2-\alpha'R\right) \frac{Z_{nm}^{2}-H_{nm}^{2}}{2R^{2}}+\left[\left(n+2\right)\left(n+1-2\alpha'R\right)+ +2\beta'R^{2}\right]\frac{Z_{nm}^{3}-H_{nm}^{3}}{6R^{3}}. \quad (18)$$

Since Z_{nm} is a constant, it only contributes to the zero-degree harmonic coefficient. The external atmospheric potential can be generated in a similar way as the external topographic potential using equation (1). It suffices just to replace the topographic harmonic coefficients with the atmospheric ones. The internal potential of the atmosphere in spherical harmonics will have the form:

$$\left(V_{int}^{a}\right)_{nm}=\frac{3}{2n+1}\frac{\rho^{a}}{\rho^{e}}\left(F_{int}^{a}\right)_{nm} \quad (19)$$

where

$$\left(F_{int}^{a}\right)_{nm} \doteq \frac{Z_{nm} - H_{nm}}{R} - \left(n - 1 - \alpha'R\right)\frac{Z_{nm}^{2} - H_{nm}^{2}}{2R^{2}} +$$
$$+ \left[\left(1 - n\right)\left(n + 2\alpha'R\right) - 2\beta'R^{2}\right]$$
$$\frac{Z_{nm}^{3} - H_{nm}^{3}}{6R^{3}} \tag{20}$$

(for mathematical derivation, see Appendix D). The internal atmospheric potential can be generated using equation (6). In a similar way as presented for the topographic bias on the gravity anomaly and disturbing potential we can write

$$\delta\Delta g_{bias}^{t}\left(P\right) \doteq \frac{GM}{R^{2}}\sum_{n,m}^{\infty}\left\{\frac{Z_{nm} - H_{nm}}{R} + \frac{3\alpha'R}{\left(2n+1\right)}\right.$$
$$\frac{Z_{nm}^{2} - H_{nm}^{2}}{2R^{2}} + \frac{Z_{nm}^{3} - H_{nm}^{3}}{6R^{3}}$$
$$\left[\left(n+2\right)\left(n-1\right) + 2\beta R^{2}\right]\Bigg\}$$
$$\left(\frac{3\rho_{0}}{\rho^{e}}\right)Y_{nm}\left(P\right), \tag{21}$$

which is the atmospheric bias for r=R on the gravity anomaly and

$$\delta V_{bias}^{a}\left(P\right) \doteq \frac{GM}{R}\sum_{n,m}^{\infty}\left\{\left(2n+1-2\alpha'R\right)\frac{Z_{nm}^{2} - H_{nm}^{2}}{2R^{2}} +\right.$$
$$+ \frac{Z_{nm}^{3} - H_{nm}^{3}}{3R^{3}}\left[\left(n^{2} + n + 1\right) -\right.$$
$$\left. -3\alpha'R + 2\beta'R^{2}\right]\Bigg\}\left[\frac{3\rho_{0}}{\left(2n+1\right)\rho^{e}}\right]$$
$$Y_{nm}\left(P\right) \tag{22}$$

is the atmospheric bias on the disturbing potential.

The atmospheric model presented by Novák (2000) is valid just to 10 km elevation from sea level. His main goal for providing such a model was just to consider the atmospheric roughness. For considering the atmospheric densities above 10 km, we can consider the standard atmospheric model (United State Standard Atmosphere, 1976); see Appendix B. We can consider atmospheric shells from 10 km to 86 km with a thickness of 100 m (710 atmospheric shells) to generate the corresponding potentials. The effect of these shells, which contributes to the zero-degree harmonic coefficient of the atmospheric potential is:

$$\left(\delta V_{ext}^{a}\right)_{0} = \frac{3}{\rho^{e}}\left\{\left(1 + \frac{Z_{j+1}}{R}\right)^{3}\rho_{j}^{a} - \left(1 + \frac{Z_{i}}{R}\right)^{3}\rho_{i}^{a} +\right.$$
$$\left. + \sum_{k=i+1}^{j}\left(1 + \frac{Z_{k}}{R}\right)^{3}\left(\rho_{k-1}^{a} - \rho_{k}^{a}\right),\right. \tag{23}$$

where, ρ_{i}^{a} is the atmospheric density of each shell, Z is upper (j) or lower (i) bound of each shell. The internal potential of these atmospheric shells, contributing with the zero-degree harmonic can be written

$$\left(\delta V_{int}^{a}\right)_{0} = \frac{3}{2\rho^{e}}\left\{\left(1 + \frac{Z_{j+1}}{R}\right)^{2}\rho_{j}^{a} - \left(1 + \frac{Z_{i}}{R}\right)^{2}\rho_{i}^{a} +\right.$$
$$\left. + \sum_{k=i+1}^{j}\left(1 + \frac{Z_{k}}{R}\right)^{2}\left(\rho_{k-1}^{a} - \rho_{k}^{a}\right)\right\} \tag{24}$$

For mathematical derivations, see Appendix C. The atmospheric potential bias due to these shells will be:

$$\left(\delta V_{bias}^{a}\right)_{0} = \frac{3}{\rho^{e}}\left\{\left(1 + \frac{z_{j+1}}{R}\right)^{2}\left(\frac{1}{2} + \frac{z_{j+1}}{R}\right)\rho_{j}^{a} -\right.$$
$$- \left(1 + \frac{z_{i}}{R}\right)^{2}\left(\frac{1}{2} + \frac{z_{i}}{R}\right)\rho_{i}^{a} +$$
$$+ \sum_{k=i+1}^{j}\left(1 + \frac{Z_{k}}{R}\right)^{2}\left(\frac{1}{2} + \frac{Z_{k}}{R}\right)$$
$$\left(\rho_{k-1}^{a} - \rho_{k}^{a}\right)\Bigg\}. \tag{25}$$

4 NON-SINGULAR EXPRESSIONS FOR THE GRAVITATIONAL GRADIENTS IN LOCAL NORTH-ORIENTED FRAME

The second-order derivatives of the potential can be written in the local north-oriented frame. This frame is defined with the z-axis pointing in the geocentric radial direction, x pointing towards the north, and y is directed to the east such that the frame becomes right-handed. It should be mentioned that the gravity gradients are directly measured in the gradiometric frame. However, one can transform them from the local to

gradiometer frame by the transformation parameters between the frames, if they are given. Let equation (1) be a potential series of expansion for topography and atmosphere. Then the non-singular expressions of the gravity gradients are given by (Petrovskaya and Vershkov, 2006)

$$V_{zz}(P) = \frac{GM}{R^3} \sum_{n,m}^{N_{max}} (n+1)(n+2) \left(\frac{R}{r}\right)^{n+3} v_{nm}$$
$$Y_{nm}(P), \tag{26}$$

$$V_{xx}(P) = \frac{GM}{R^3} \sum_{n,m}^{N_{max}} \left(\frac{R}{r}\right)^{n+3} v_{nm} Q_m(\lambda) \{ a_{nm}$$
$$\overline{P}_{n,|m|-2} + \left[b_{nm} - (n+1)(n+2) \right]$$
$$\overline{P}_{n,|m|} + c_{nm} \overline{P}_{n,|m|+2} \} \tag{27}$$

$$V_{yy}(P) = \frac{GM}{R^3} \sum_{n,m}^{N_{max}} \left(\frac{R}{r}\right)^{n+3} v_{nm} Q_m(\lambda) \Big[a_{nm}$$
$$\overline{P}_{n,|m|-2} + b_{nm} \overline{P}_{n,|m|} + c_{nm} \overline{P}_{n,|m|+2} \Big], \tag{28}$$

$$V_{xy}(P) = \frac{GM}{R^3} \sum_{n,m}^{N_{max}} \left(\frac{R}{r}\right)^{n+3} v_{nm} Q_{-m}(\lambda) \Big[d_{nm}$$
$$\overline{P}_{n-1,|m|-2} + g_{nm} \overline{P}_{n-1,|m|} + h_{nm} \overline{P}_{n-1,|m|+2} \Big]$$
$$m \neq 0 \tag{29}$$

$$V_{xz}(P) = \frac{GM}{R^3} \sum_{n,m}^{N_{max}} \left(\frac{R}{r}\right)^{n+3} v_{nm} Q_m(\lambda) \Big[\beta_{nm}$$
$$\overline{P}_{n,|m|-1} + \gamma_{nm} \overline{P}_{n,|m|+1} \Big] \tag{30}$$

$$V_{yz}(P) = \frac{GM}{R^3} \sum_{n,m}^{N_{max}} \left(\frac{R}{r}\right)^{n+3} v_{nm} Q_{-m}(\lambda) \Big[\mu_{nm}$$
$$\overline{P}_{n-1,|m|-1} + \nu_{nm} \overline{P}_{n-1,|m|+1} \Big], m \neq 0 \tag{31}$$

where $\overline{P}_{n|m|} = \overline{P}_{n|m|}(\cos\theta)$ and the constant coefficients a_{nm}, b_{nm}, c_{nm}, d_{nm}, g_{nm}, h_{nm}, β_{nm}, γ_{nm}, μ_{nm}, and ν_{nm} are presented in

Appendix A. N_{max} is the maximum degree and order of the spherical harmonic expansion. Some of these expressions do not include zero- and/or first-degree harmonics. For more details, see Eshagh and Sjöberg (2008).

5 NUMERICAL STUDIES IN IRAN

We now consider the region limited by latitudes $25°$ N and $40°$ N and longitudes between $44°$ E and $64°$ E for some numerical investigations. The EIGEN-Gl04c geopotential model (Förste et al. 2005), obtained from orbital analysis of the combination of GRACE and LAGEOS satellite missions as well as gravity and altimetry surface data, was used to generate the spherical harmonic coefficients of the geoidal height and its second and third powers. The global spherical harmonic coefficients of the topographic height including its second and third powers, the latter extracted from SRTM satellite images (Wieczorek, 2007), was employed in the harmonic expansion to degree and order 360 for our computations. A MATLAB program code has been written, which computes the spherical harmonic coefficients of topographic and atmospheric potentials. These potential models are used to compute the second order gradients in the local north-oriented reference frame according to the formulas of the previous section. The program was used to generate maps of the topographic and atmospheric effects at the altitude of 250 km, the altitude of GOCE over Iran, as well as their statistics. In the following these effects are presented in maps and tables.

Table 1. Statistics of topographic effects on GOCE gravity gradients in Iran, Unit:1 E.

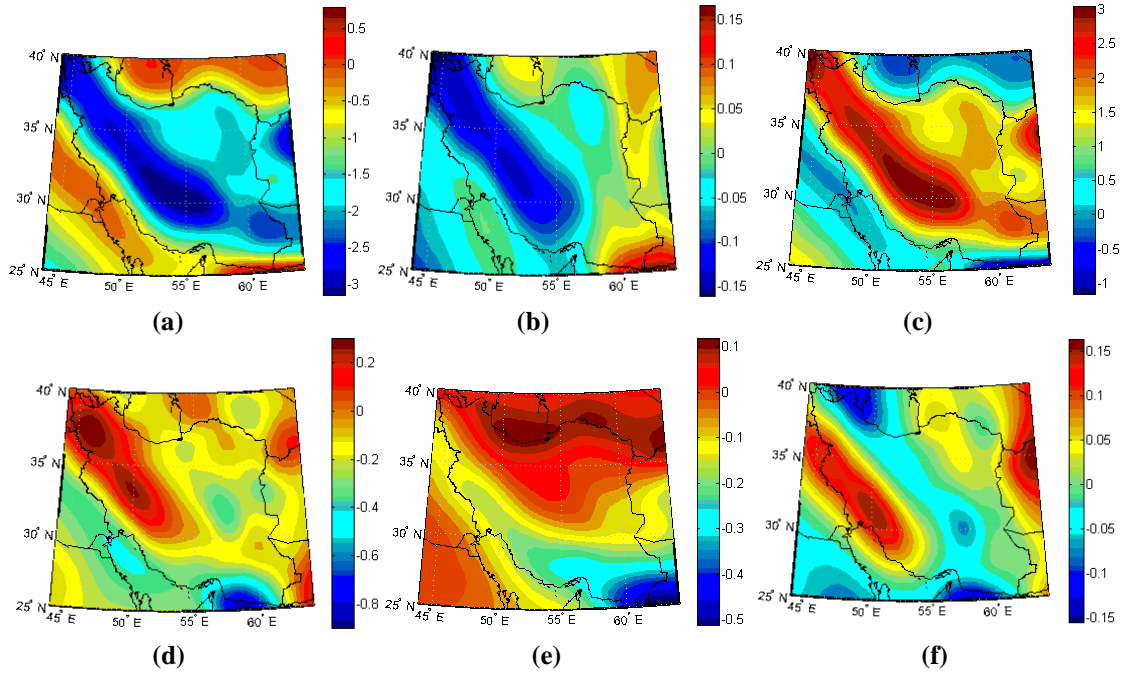|	Max	Mean	Min	Standard deviation
V_{xx}^t	0.59	-0.65	-2.60	± 0.68
V_{yy}^t	1.06	0.01	-1.16	± 0.48
V_{zz}^t	2.64	0.64	-0.76	± 0.94
V_{xy}^t	0.98	-0.14	-0.89	± 0.41
V_{xz}^t	1.72	-0.10	-1.94	± 0.92
V_{yz}^t	1.69	0.20	-1.35	± 0.58

Figure 1. Topographic effects in Iran in local north-oriented frame, Unit:1 E.

Figures 1 (a), (b), (c), (d), (e), and (f) present the gravitational gradients V_{xx}^t, V_{yy}^t, V_{zz}^t, V_{xy}^t, V_{xz}^t, and V_{yz}^t, respectively. As can be seen, they are all in the order of a few Eötvös (1E=0.1mGalkm^{-1}). In proper SI units, the Eötvös unit equals 10^{-9} s^{-2}. Some statistics of our results are given in table 1. It shows that the north-south and vertical gradients are larger than any of the other gradients, as they include zero- and first-degree harmonics which is not the case for the others.

The significant topographic features in Iran are extended from the south to the north-west part and along the Iranian border to Turkey, Iraq, and Azerbaijan; and the Alborz mountains. The highest elevation in the SRTM data set is 3000 m in this region. As can be expected, the topographic effects are clearly related to topography and reduce quickly as one moves away from such areas. This result is also obvious from table 4. The maximum mean effect of the topographic effect is related to V_{zz}^t and equals 2.64 E of gravitational gradients and the minimum mean effect is about -0.76 E. It means that the topographic effect in this region is considerable, and should be regarded or removed before doing regional gravity field determination or downward continuation of GOCE data. Both downward continuation and geoid computation need, or are at least simplified, by the removal of the effect of the topography.

The topographic effect can be geophysically interpreted too. As we know V_{xx} is the second-order derivative of the topographic potential (northward), and it presents the curvature of the topographic surface, or, in other words, it shows the convexity and the concavity of the topographic surface. In figure 1a every massive part of the topography shows the most concave parts of the topographic surface (negative) and the most convex parts of the topographic masses relate to the topographic lateral boundaries. V_{xx} is the second order derivative along the northern direction and it is obvious that the two most concave parts are in the northern and southern parts of the topography and the convex part on the topographic feature. A similar explanation can be made for V_{yy}. V_{zz} also presents the curvature of gravity, but along the radial direction, and it is clear that the most variation of the gradient of the gravity is related to the most massive parts. This is why V_{zz} is used in exploration for determining the depth. V_{xz} and

V_{yz} have similar interpretations as the components of the deflection of the vertical. They show lateral boundaries of the features, too, but on one side (depending on the direction, north-south or east-west) of the topographic feature they are positive/negative, but in the other part they are negative/positive. Also, they present the torsion of the plumb line; see Moritz and Hofmann-Wollenhof (1993). V_{xy} has a different and more difficult interpretation since it presents the torsions of the topographic surface; see figure 2d. For more details about the geophysical interpretations of gravity gradients we refer to

Pawlowski and Prieto (1997), Pawlowski (1998), Mickus and Hinojosa (2001) and Li (2001a, 2001b and 2001c).

Figures 2 (a), (b), (c), (d), (e), and (f) present V_{xx}^a, V_{yy}^a, V_{zz}^a, V_{xy}^a, V_{xz}^a, and V_{yz}^a, respectively. As can be seen, the atmospheric effects are very small relative to the topographic effects. They are in the order of mE. The maximum mean value of atmospheric effect is about 4.82 mE and its minimum is about -0.5 mE, suggesting that, this effect can usually be neglected for the present type of geodetic applications.
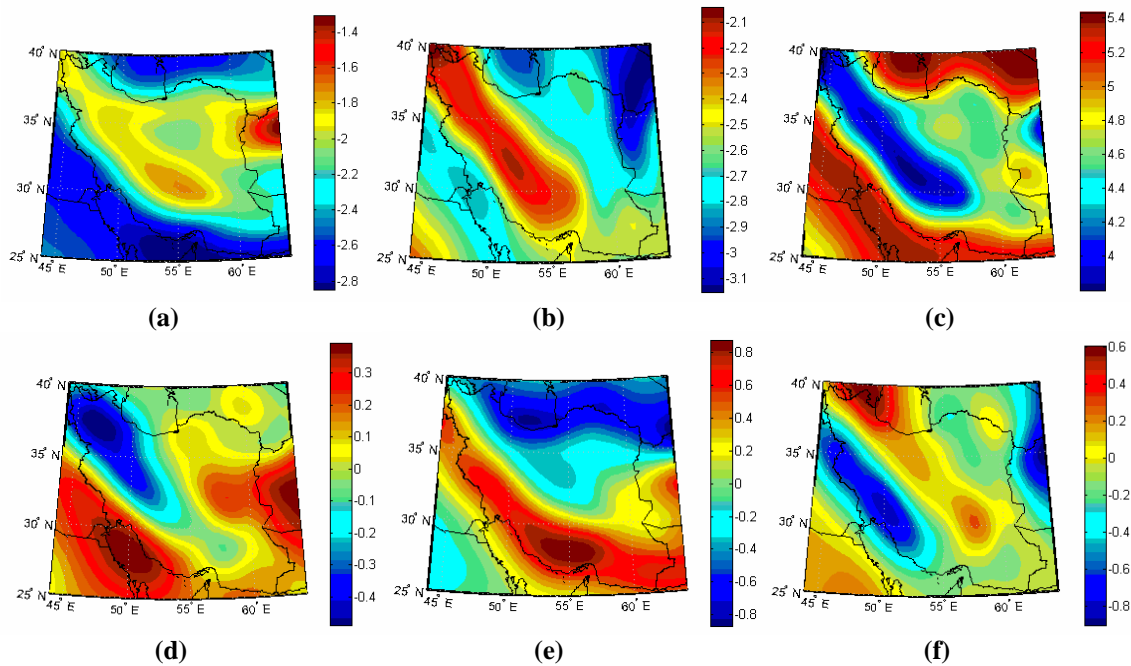

Figure 2. Atmospheric effects in Iran in the local north-oriented frame, Unit: mE.

Table 2. Statistics of atmospheric effects on GOCE gravity gradients in Iran, Unit: 1 mE.

	Max	Mean	Min	Standard deviation
V_{xx}^a	-1.20	-2.23	-2.86	± 0.35
V_{yy}^a	-1.97	-2.59	-3.16	± 0.25
V_{zz}^a	5.53	4.82	3.78	± 0.48
V_{xy}^a	0.45	0.07	-0.50	± 0.21
V_{xz}^a	0.99	0.06	-0.89	± 0.47
V_{yz}^a	0.70	-0.10	-0.91	± 0.30

Most presented figures demonstrate high correlations between some of the gradients and topographic height; cf. the topographic map of figure 3, computed by the same topographic data that was used for the determination of the gradients above (i.e. the spherical harmonic coefficients of the SRTM global topographic model to degree and order 360).
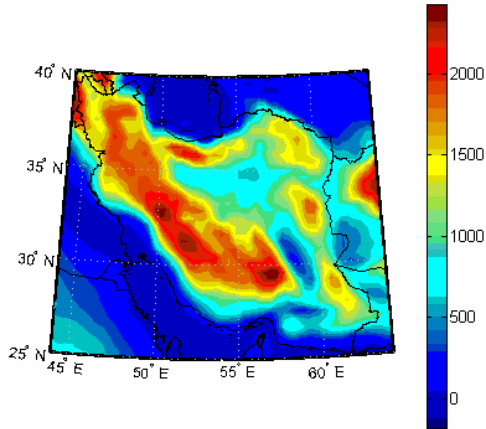

Figure 3. Long-wavelength topography of Iran in units of meters, obtained by the spherical harmonic coefficients of the SRTM global model.

The correlations between topographic and atmospheric effects are presented in table 3 showing that some of the gradients $(V_{xx}, V_{yy}, V_{zz}, V_{xy}, V_{xz}, V_{yz})$ are strongly correlated with topographic height.

Table 3. Correlation coefficients between topography, and topographic, atmospheric effects in Iran.

	Topographic effect	Atmospheric effect
V_{xx}	-0.81	0.80
V_{yy}	-0.63	0.60
V_{zz}	0.91	-0.90
V_{xy}	0.52	-0.51
V_{xz}	-0.10	0.10
V_{yz}	0.08	-0.08

It is also interesting to note that the topographic and atmospheric effects have approximately the same correlations with the topographic height, but with opposite signs. This can be explained by the fact that the atmosphere does not exist where there is topography. The least correlations with the topography are related to V_{xz} and V_{yz} in both effects.

6 CONCLUSIONS

In this paper external and internal potentials of the topographic and atmospheric masses are presented in spherical harmonic coefficients. The internal and the biases of topographic and atmospheric potentials were formulated. Novák's approach was considered for the atmospheric potential. The atmospheric potential up to 10 km elevation above the sea surface is considered by Novák's density model and for the atmospheric masses above 10 km the standard atmospheric model was used to generate the potential. We have presented the direct topographic and atmospheric effects on the GOCE gradiometric over Iran. These effects on GOCE flying at the altitude of 250 km, were computed and presented in the local north-oriented frame in some maps. The maximum mean effect of the topographic gravitational gradients equals 2.63 E. It means that the topographic effect in this region has a very considerable impact on the GOCE data. The direct atmospheric effect is generally negligible in practical geodetic applications unless precise validation or calibration of GOCE gradiometric data is needed. We showed also, that some effects are strongly correlated with topographic height below the computation point. A simple geophysical interpretation was made for the direct topographic effect on GOCE gravity gradiometry data. The interpretations are promising in the investigation of the GOCE data in geophysical aspects and crustal studies.

APPENDIX A

The constant coefficients related to equation (11)-(15) are

$$a_{nm} = \begin{cases} 0 & |m| = 0,1 \\ \dfrac{\sqrt{1+\delta_{|m|,2}}}{4}\sqrt{n^2-\left(|m|-1\right)^2}\times \\ \sqrt{n+|m|}\sqrt{n-|m|+2} & 2 \le |m| \le n \end{cases}$$

(A.1)

$$b_{nm} = \begin{cases} \dfrac{\left(n+|m|+1\right)\left(n+|m|+2\right)}{2\left(|m|+1\right)} & |m| = 0,1 \\ \dfrac{n^2+m^2+3n+2}{2} & 2 \le |m| \le n \end{cases}$$

(A.2)

$$c_{nm} = \begin{cases} \dfrac{\sqrt{1+\delta_{|m|,2}}}{4}\sqrt{n^2-\left(|m|+1\right)^2}\sqrt{n-|m|}\times \\ \sqrt{n+|m|+2}, & |m| = 0,1 \\ \dfrac{1}{4}\sqrt{n^2-\left(|m|+1\right)^2}\sqrt{n-|m|}\sqrt{n+|m|+2}, \\ \hspace{4cm} 2 \le |m| \le n \end{cases}$$

(A.3)

$$d_{nm} = \begin{cases} 0 & |m| = 1 \\ -\dfrac{m}{4|m|}\sqrt{\dfrac{2n+1}{2n-1}}\sqrt{1+\delta_{|m|,2}}\times \\ \times\sqrt{n^2-\left(|m|-1\right)^2}\sqrt{n+|m|}\sqrt{n+|m|-2}, \\ \hspace{4cm} 2 \le |m| \le n \end{cases}$$

(A.4)

$$g_{nm} = \begin{cases} \dfrac{m}{4|m|}\sqrt{\dfrac{2n+1}{2n-1}}\sqrt{n+1}\sqrt{n-1}\left(n+2\right), \\ \hspace{4cm} |m| = 1 \\ \dfrac{m}{2}\sqrt{\dfrac{2n+1}{2n-1}}\sqrt{n+|m|}\sqrt{n-|m|}, \\ \hspace{4cm} 2 \le |m| \le n \end{cases}$$

(A.5)

$$h_{nm} = \begin{cases} \dfrac{m}{4|m|}\sqrt{\dfrac{2n+1}{2n-1}}\sqrt{n-3}\sqrt{n-2}\times \\ \sqrt{n-1}\sqrt{n+2}, & |m| = 1 \\ \dfrac{m}{4|m|}\sqrt{\dfrac{2n+1}{2n-1}}\sqrt{n^2-\left(|m|+1\right)^2}\times \\ \sqrt{n-|m|}\sqrt{n-|m|-2}, & 2 \le |m| \le n \end{cases}$$

(A.6)

$$\beta_{n,m} = \begin{cases} 0 & |m| = 0 \\ \dfrac{n+2}{2}\sqrt{1+\delta_{|m|,1}}\sqrt{n+|m|}\times \\ \sqrt{n-|m|+1}, & 1 \le |m| \le n \end{cases}$$

(A.7)

$$\gamma_{nm} = \begin{cases} -\left(n+2\right)\sqrt{\dfrac{n\left(n+1\right)}{2}}, & |m| = 0 \\ -\dfrac{\left(n+2\right)}{2}\sqrt{n-|m|}\sqrt{n+|m|+1}, \\ 1 \le |m| \le n \end{cases}$$

(A.8)

$$\mu_{nm} = -\dfrac{m}{|m|}\left(\dfrac{n+2}{2}\right)\sqrt{\dfrac{2n+1}{2n-1}}\sqrt{1+\delta_{|m|,1}}\times$$
$$\sqrt{n+|m|}\sqrt{n+|m|-1} \qquad \text{(A.9)}$$

$$v_{nm} = -\dfrac{m}{|m|}\left(\dfrac{n+2}{2}\right)\sqrt{\dfrac{2n+1}{2n-1}}\sqrt{n-|m|}\times$$
$$\sqrt{n-|m|-1} \qquad \text{(A.10)}$$

where δ is Kroneker's delta.

APPENDIX B
STANDRD ATMOSPHERIC MODEL

Among different atmospheric models one which is frequently used is the standard atmospheric density model (United State Standard Atmosphere, 1976) as

$$\rho^a\left(H\right)=\frac{\mu P\left(H\right)}{\kappa T\left(H\right)} \tag{B.1}$$

where $\kappa=8314.32$ (N m km^{-1} K^{-1}) is the universal gas constant, $\mu=28.9644$ (kgkmol^{-1}) is mean molecular weight of the atmospheric masses at sea level, P=101325(Nm^{-2}) is the atmospheric pressure and T=288.12 K the molecular-scale temperature of the atmosphere in K.

In this model the atmosphere between topography and height at 86 km is divided into 7 layers, in which the molecular-scale temperature and atmospheric pressure are modeled as:

$$\forall i=1,2,...,7:\quad T\left(H\right)=T_i+\tau_i\left(H-H_i\right) \tag{B.2}$$

$$\forall i\in\{1,3,4,6,7\}:P\left(H\right)=P_i\left[\frac{T_i}{T\left(H\right)}\right]^{\frac{g\mu}{\kappa\tau_i}} \tag{B.3}$$

$$\forall i\in\{2,5\}:P\left(H\right)=P_i\exp\left[\frac{-g\mu\left(H-H_i\right)}{\kappa\tau_i}\right] \tag{B.4}$$

where H is the height within and H_i is the reference height of each layer, T_i is the reference value of the molecular-scale temperature for the i-th layer, τ_i is the molecular-scale temperature gradient; cf. Table B1., P_i stands for the reference pressure, g=9.80665 ms^{-2} is the gravity value at sea level. The molecular temperature gradient of each layer is presented in table B1.

Table B1. Molecular temperature gradients, Novák (2000).

Layer	Height (km)	τ_i (K km^{-1})
1	0-11	-6.5
2	11-20	+0.0
3	20-32	+1.0
4	32-48	+2.8
5	48-51	+0.0
6	51-71	-2.8
7	71-86	-2.0

APPENDIX C
POTENTIAL OF THE ATMOSPHERIC SHELLS

The external type of the potential of a spherical shell is (see also Sjöberg, 2007, equation 16)

$$V_{ext}^a\left(P\right)=\frac{4\pi G\rho_i^a}{r_P}\int_{R+Z_i}^{R+Z_{i+1}}r_Q^2dr_Q=$$
$$=\frac{4\pi G\rho_i^a}{3r_P}\left[\left(R+Z_{i+1}\right)^3-\left(R+Z_i\right)^3\right] \tag{C.1}$$

This is the potential of atmospheric shell with density ρ_i^a. Equation (C.1) can also be written

$$V_{ext}^a\left(P\right)=\frac{GM}{R}\frac{R}{r_P}\frac{3\rho_i^a}{\rho^e}\left[\left(R+Z_{i+1}\right)^3-\left(R+Z_i\right)^3\right] \tag{C.2}$$

yielding

$$\left(\delta V_{ext}^a\right)_0=\frac{\rho_i^a}{\rho^e}\left[\left(1+\frac{Z_{i+1}}{R}\right)^3-\left(1+\frac{Z_i}{R}\right)^3\right], \tag{C.3}$$

This potential contributes only to the zero-degree harmonic coefficient is related to one atmospheric shell confined between Z_{i+1} and Z_i elevations. The total potential of all shells is a summation of potential of each atmospheric shell as in equation (7).

In a similar manner, the internal type of the potential of a spherical shell is; see Sjöberg (2007)

$$\left(\delta V_{int}^a\right)_0=4\pi G\rho_i^a\int_{R+Z_i}^{R+Z_{i+1}}r_Qdr_Q=$$
$$2\pi G\rho_i^a\left[\left(R+Z_{i+1}\right)^2-\left(R+Z_i\right)^2\right], \tag{C.4}$$

Also

$$\left(\delta V_{int}^a\right)_0=\frac{GM}{R}\frac{3\rho_i^a}{2\rho_e}\left[\left(R+Z_{i+1}\right)^2-\left(R+Z_i\right)^2\right] \tag{C.5}$$

and the summation of all the atmospheric shells can be written in the form of equation (24).

APPENDIX D

The atmospheric potential is expressed according to the well-known Newtonian volume integral as

$$V^a(P) = G \iint_\sigma \int_{r_S}^{r_Z} \rho^a(r_Q) \frac{r_Q^2 dr_Q}{l_{PQ}} d\sigma, \qquad (D.1)$$

where, G is the Newtonian gravitational constant, $V^a(P)$ stands for the atmospheric potential at point P, $\rho^a(r_Q)$ is the atmospheric density function, at point Q (integration point), σ is the full solid angle of integration, r_S and r_Z are the topographic surface, and the upper limit of the atmosphere, l_{PQ} is the distance between computation point P and integration point Q. dr_Q and $d\sigma$ are the radial and horizontal integration elements, respectively. In order to obtain the direct atmospheric effect $1/l_{PQ}$ is expanded into Legendre series of external type as:

$$\frac{1}{l_{PQ}} = \frac{1}{r_P} \sum_{n=0}^{\infty} \left(\frac{r_P}{r_Q}\right)^{n+1} P_n(\cos\psi_{PQ}), \qquad (D.2)$$

Inserting equation (16a) and (D.2) into equation (D.1) and considering $r_Z = R + Z$ and $r_S = R + H$

$$V_{ext}^a(P) = G\rho_0 \sum_{n=0}^{\infty} r_P^n \iint_\sigma \int_{R+H}^{R+Z} \left[1 + \alpha'(r_Q - R) + \right.$$
$$\left. + \beta'(r_Q - R)^2\right] r_Q^{-n+1} dr_Q$$
$$P_n(\cos\psi_{PQ}) d\sigma. \qquad (D.3)$$

The radial integral can be separately written as

$$\int_{R+H}^{R+Z} \left[1 + \alpha'(r_Q - R) + \beta'(r_Q - R)^2\right] r_Q^{-n+1} dr_Q =$$
$$(1 - \alpha R + \beta R^2) \int_{R+H}^{R+Z} r_Q^{-n+1} dr_Q + (\alpha - 2R\beta)$$
$$\int_{R+H}^{R+Z} r_Q^{-n+2} dr_Q + \beta \int_{R+H}^{R+Z} r_Q^{-n+3} dr_Q = I, \qquad (D.4)$$

and solution of this integral will be

$$I_n = \frac{(1 - \alpha'R + \beta'R^2)R^{-n+2}}{-n+2} \left[\left(1 + \frac{Z}{R}\right)^{-n+2} - \right.$$
$$\left. - \left(1 + \frac{H}{R}\right)^{-n+2}\right] + \frac{(\alpha' - 2\beta'R)R^{-n+3}}{-n+3}$$
$$\left[\left(1 + \frac{Z}{R}\right)^{-n+3} - \left(1 + \frac{H}{R}\right)^{-n+3}\right] + \frac{\beta'R^{-n+4}}{-n+4}$$
$$\left[\left(1 + \frac{Z}{R}\right)^{-n+4} - \left(1 + \frac{H}{R}\right)^{-n+4}\right] \qquad (D.5)$$

Using the Taylor expansion for the above terms in the square brackets up to fourth order the singularities in Equation (D.5) are cancelled out; and after long derivations we obtain

$$I_n = R^{-n+2} F_{int}^a(Q) \qquad (D.6)$$

$$F_{int}^a(Q) = \left\{\frac{Z-H}{R} - (n-1-\alpha'R)\frac{Z^2 - H^2}{2R^2} - \right.$$
$$- \left[(1-n)(n+2\alpha'R) - 2\beta'R^2\right]$$
$$\left. \frac{Z^3 - H^3}{6R^3}\right\} \qquad (D.7)$$

By substituting

$$V_{int}^a(P) = GR^2\rho_0 \sum_{n=0}^{\infty} \left(\frac{r_P}{R}\right)^n \iint_\sigma F_{int}^a(Q)$$
$$P_n(\cos\psi_{PQ}) d\sigma \qquad (D.8)$$

According to the addition theorem of the fully-normalized spherical harmonics we have

$$P_n(\cos\psi_{PQ}) = \frac{1}{2n+1} \sum_{m=-n}^{n} Y_{n,m}(Q) Y_{n,m}(P) \qquad (D.9)$$

where

$$\iint_\sigma Y_{nm}(Q) Y_{n'm'}(P) d\sigma = 4\pi \delta_{nn'} \delta_{mm'}, \qquad (D.10)$$

yielding

$$V_{int}^a (P) = \frac{GM}{R} \sum_{n=0}^{\infty} \left(\frac{r_P}{R}\right)^n \sum_{n=-m}^{m} \left(v_{int}^a\right)_{nm} Y_{nm}(P)$$

(D.11)

where

$$GM = 4\pi R^3 \rho_e G / 3 ,$$

(D.12)

$$\left(V_{int}^a\right)_{nm} = \frac{3\rho_0}{(2n+1)\rho^e} \left(F_{int}^a\right)_{nm}$$

(D.13)

and

$$\left(F_{int}^a\right)_{nm} = \left\{ \frac{Z_{nm} - H_{nm}}{R} - (n - 1 - \alpha' R) \frac{Z_{nm}^2 - H_{nm}^2}{2R^2} \right.$$

$$\frac{Z_{nm}^3 - H_{nm}^3}{6R^3}$$

(D.14)

REFERENCES

Ditmar, P., Klees, R., and Kostenko, F., 2003, Fast and accurate computation of spherical harmonics coefficients from satellite gravity gradiometry data, J. Geodesy, **76**, 690-705.

Ecker, E., and Mittermayer, E., 1969, Gravity corrections for the influence of the atmosphere. Boll Geofis Teor Appl., **11**, 70-80.

Eshagh, M., and Sjöberg, L. E., 2008, Topographic and atmospheric effects on GOCE gradiometric data in a local north-oriented frame: A case study in Fennoscandia and Iran, Stud. Geophys. Geodesy, (Accepted).

Förste, C., Flechtner, F., Schmidt, R., Meyer, U., Stubenvoll, R., Barthelmes, F., König, R., Neumayer, K. H., Rothacher, M., Reigber, Ch., Biancale, R., Bruinsma, S., Lemoine, J. M., Raimondo, J. C., 2005, A new high resolution global gravity model derived from combination of GRACE and CHAMP mission and altimetry-gravimetry surface gravity data, Poster g004 EGU-A-04561 presented at EGU General assembly 2005, Vienna, Austria, 24-29, April 2005.

Heiskanen, W. A., and Moritz, H., 1967, Physical geodesy, W. H. Freeman and Co., San Francisco.

Koop, R., 1993, Global gravity field modeling using satellite gravity gradiometry. Publ Geodesy, New series, No. 38. Netherland Geodetic Commission, Delft.

Klees, R., Koop, R., Visser, P., van den IJssel J, 2000, Efficient gravity field recovery from GOCE gravity gradient observations, J. Geodesy, **74**, 561-571.

Lambeck, K., 1988, Geophysical geodesy, the Slow Deformations of the Earth. Clarendon, Oxford University Press, New York.

Lemoine, F. G., Kenyon, S. C., Factor, J. K., Trimmer, R. G., Pavlis, N. K., ChinnDs, Cox C. M, Klosko, S. M, Luthck,e S. B., Torrence, M. H., Wang, Y. M., Williamson, R. G., Pavlis, E. C., Rapp, R. H., and Olson, T. R., 1998, Geopotential model EGM96. NASA/TP-1998-206861. Goddard Space Flight Center, Greenbelt.

Li X., 2001a, Vertical resolution: Gravity versus vertical gravity gradient. Lead. Edge, **20**, 901-904.

Li Y., 2001b Processing gravity gradiometer data using an equivalent source technique. Publications in center for gravity, Electrical and Magnetic studies, Dept. Geophysics, Colorado School of Mines.

Li Y., 2001c, 3-D Inversion of gravity gradiometer data. Publications in center fro gravity, Electrical and Magnetic studies, Dept. Geophysics, Colorado School of Mines.

Martinec, Z., 2003, Green's function solution to spherical gradiometric boundary-value problems, J. Geodesy, **77**, 41-49.

Mickus, K. L., and Hinojosa, J. H., 2001, The complete gravity gradient tensor derived from the vertical component of gravity: a Fourier transform technique. Journal of Applied Geophysics, **46**, 159-274.

Moritz, H., and Hofmann-Wollenhof, B., 1993, Geometry, Relativity and Geodesy, Wichman, Karlsruhe.

Novák, P, 2000, Evaluation of gravity data for the Stokes-Helmert solution to the geodetic boundary-value problem. Technical Report 207, Department of Geodesy and Geomatics Engineering, University of New Brunswick, Fredericton, Canada.

Novák, P., 2007, Integral inversion of SST data of type GRACE, Stud. Geophys. Geodesy, **51**, 351-367.

Novák, P., and Grafarend, E. W., 2006, The effect of topographic and atmospheric masses on spaceborne gravimetric and gradiometric data, Stud. Geophys. Geodesy, **50**, 549-582.

Pawlowski, B., 1998, Gravity gradiometry in resource exploration: Lead. Edge, **17**, 51-52.

Pawlowski, R., and Prieto, C., 1997, Gravity gradiometry in natural resource exploration.

IGC Footnote Series, Volume 4, Number 1.

Petrovkaya, M. S., and Vershkov, A. N., 2006, Non-singular expressions for the gravity gradients in the local north-oriented and orbital reference frames, J. Geodesy, **80**, 117-127.

Reed, G. B., 1973, Application of kinematical geodesy for determining the short wave lenGGTh components of the gravity field by satellite gradiometry. Ohio State University, Dept of Geod. Science, Rep. No. 201, Columbus, Ohio.

Rummel, R., 1975, Downward continuation of gravity information from satellite to satellite tracking or satellite gradiometry in local areas, Report N0. 221, Grant No. NGR 36-008-161 OSURF project No. 3210, Ohio State University, Columbus Ohio.

Rummel, R., Sanso, F., van Gelderen, M., Koop R., Schrama, E., Brovelli, M., Migiliaccio, F., and Sacerdote, F., 1993, Spherical harmonic analysis of satellite gradiometry. Publ Geodesy, New Series, No. 39 Netherlands Geodetic Commission, Delft.

Sjöberg, L. E., 1984, Least squares modification of Stokes' and Vening Meinesz' formulas by accounting for truncation and potential coefficient errors: Manuscr. Geodaet., **9**, 209-229

Sjöberg, L. E., 1986, The Modification of Stokes' and Hotine's Formulas A Comparison. Proceedings of the International Symposium. The Figure and Dynamics of the Earth, Moon and Planets, Prague, 15 19 September, 1986. Proc. 10th Gen. Meeting of Nordic Geodetic Commission, pp. 268 278, Helsinki

Sjöberg, L. E., 1991, Refined least squares modification of Stokes' formula. Presented to IAG Scientific Meeting "The Challenge of the cm Geoid Strategies and State of the Art". XIX General Assembly of the IUGG Vancouver, Canada, August 9 22, 1987 (13 pages). Manuscripta Geodetica, **6**, 367-375.

Sjöberg, L. E., 2007, the topographic bias by analytical continuation in physical geodesy, J. Geodesy, **81**, 345-350.

Sneeuw, N., 1992, Representation coefficients and their use in satellite geodesy, Manuscr, Geodesy, **17**, 117-123.

Sneeuw, N., 2000, A semi-analytical approach to gravity field analysis from satellite observations. Reihe C, Helft Nr. 527, Deutsche Geodätische Kommission, München.

Sneeuw, N., Dorobantu, R., Gerlach, Mueller J., Oberndorfer, H., Rummel, R., Koop, R., Visser, P., Hoyng, P., Selig, A., Smit, M., 2001, Simulation of the GOCE gravity field mission. In: Bensiolini B (ed) IV Hotine-Marussi symposium on mathematical geodesy. IAG Symposia, vol 122, Springer, Berlin Heidelberg New York pp. 14-20.

United State Standard Atmosphere 1976, Joint model of the National Oceanic and Atmospheric administration, national aeronautics and space administration and United States Air Force, Washington, D.C.

Wallace, J. M., and Hobbs, P. V., 1977, Atmospheric Science-An Introductory Survey, Academic press, New York.

Wieczorek, M. A., 2007, The gravity and topography of the terrestrial planets, Treatise Geophys., in press